Available online at www.sciencedirect.com
SCIENCE DIRECT®
Materials Chemistry and Physics 89 (2005) 406–411
MATERIALS CHEMISTRY AND PHYSICS
www.elsevier.com/locate/matchemphys

Effect of La^{3+} substitution on the structural, electrical and electrochemical properties of strontium ferrite by citrate combustion method

C.O. Augustin*, R. Kalai Selvan, R. Nagaraj, L. John Berchmans

Central Electrochemical Research Institute, Karaikudi 630 006, India

Received 2 July 2004; accepted 21 September 2004

Abstract

The La^{3+} substituted nanocrystalline strontium ferrite has been prepared by citrate combustion method using metal nitrate salts as cation precursors and citric acid as a fuel. The structural characteristics of the compounds have been evaluated using XRD and FTIR. The existence of the single-phase perovskite structure with nanocrystalline size has been confirmed from the X-ray powder diffraction patterns. The stretching and bending vibrations of the metal cations are confirmed from the FTIR spectra. The electrical conductivity of the materials is found to increase with increasing temperature measured by using a modified four-probe technique. The electrochemical behavior has been studied by using potentiostatic polarization method in KOH solutions at two different concentrations of 1 and 2 M. From the polarization studies it has been found that the material $La_{0.4}Sr_{0.6}FeO_3$ gives the lowest corrosion rate of 0.001 mmpy in 1 M KOH solution.

Keywords: Oxides; Chemical synthesis; X-ray diffraction; Fourier transform infrared spectroscopy; Electrical conductivity; Electrochemical techniques

1. Introduction

The elements with variable valence are substituted in A-site or B-site of the ABO_3 perovskite structure to improve the structural and electrical properties required for specific areas of applications. The strontium substituted $LaMO_3$ (M = Fe, Mn, Cr, Co, Ni, Sc) have good electrical conductivity, electrocatalytic activity, thermal stability, chemical stability at oxidation and reduction reactions at high temperatures. Therefore, they have been used as electrodes [1] and electrolyte materials for solid oxide fuel cells [2], secondary batteries [3], magnetohydrodynamic power generators [4] potential catalytic materials in place of noble metals [5]. Recently, the unsubstituted $SrFeO_{3-\delta}$ has been prepared by co-precipitation method, envisaged to use as an inert anode for the extractive metallurgical purposes [6]. By this, green house gases such as CO, CO_2 and CF_4, could be eliminated enabling an eco-friendly production of metals. Many synthetic methods are available for preparing new materials [7], by which nanosized powders are seldom obtained. Among these, citrate combustion process is potentially advantageous in comparison with other methods for achieving homogeneous mixing of the compounds on the atomic scale, lower processing temperature, high purity of the synthesized materials, good control of stoichiometry, desired particle size distribution with high surface area and better sinterability.

In the present investigation, nanocrystalline $La_xSr_{1-x}FeO_3$ ($x = 0.0, 0.2, 0.4, 0.6, 0.8$) was prepared by using novel citrate combustion method [8]. The structural, electrical and electrochemical properties of all the samples were investigated by using various techniques with a view to explore their applications as green electrode materials.

2. Experimental

Lanthanum substituted strontiumorthoferrite was prepared by using citrate combustion process with required amounts of high purity lanthanum nitrate, strontium nitrate, ferric nitrate and citric acid as starting materials. The stoi-

* Corresponding author. Tel.: +91 4565 227550; fax: +91 4565 227713/79.
E-mail address: caugustin@rediffmail.com (C.O. Augustin).

0254-0584/$ – see front matter © 2004 Elsevier B.V. All rights reserved.
doi:10.1016/j.matchemphys.2004.09.028

chiometric redox reactions between metal nitrates and citric acid to produce one mole of $SrFeO_{3-\delta}$ would require 2:1 molar ratios as calculated from the following equation

$$x\mathrm{La(NO_3)_3} + (1-x)\mathrm{Sr(NO_3)_2} + \mathrm{Fe(NO_3)\cdot 9H_2O} + \mathrm{C_6H_8O_7\cdot H_2O} \rightarrow \mathrm{La_xSr_{1-x}FeO_3} + 6\mathrm{CO_2} + 14\mathrm{H_2O} + 0.5(5+x)\mathrm{N_2} + 0.5(3x+2)\mathrm{O_2} \quad (1)$$

The calculated quantities of nitrate salts were dissolved in triple distilled water and required amounts of citric acid were added as chelating agent. Dilute aqueous ammonia was poured slowly into the nitrate–citrate mixture to adjust the pH to 6.5. The mixed solution was heated at about 100 °C for 5 h with uniform stirring and evaporated to obtain a highly viscous gel denoted as precursors. The obtained gel was placed in a hot plate maintained at a temperature of 300 °C, the gel was swelled and ignited with an evolution of large amounts of gaseous products, resulting the desired ferrite in the form of foamy powder. The powder was then powdered and compacted at a pressure of 3.5 tons cm^{-2} into 1 and 2.5 cm diameter pellets under identical conditions. The pellets were sintered at 1000 °C in air for 50 h. DC electrical conductivity of the sintered electrodes was measured as a function of temperature up to 1000 °C using a modified four-probe method. The crystalline phases of the prepared powders were identified by powder X-ray diffraction technique using an X-ray diffractometer CuKα radiation (λ = 0.15406 nm). The FTIR spectra of the samples were recorded as KBr discs in the range of 400–1000 cm^{-1} by using FTIR, Perkin-Elmer, UK Paragon-500. Electrochemical polarization studies were performed using Volta lab—PGA201 potentiostat/galvanostat. A conventional three-electrode system was used for the electrochemical measurements. A 'Pt' foil was used as a counter electrode; a saturated Hg/HgO/1 M KOH electrode was used as the reference electrode. The sintered 1 cm diameter with 0.5 cm thickness bulk material was used as the working electrode.

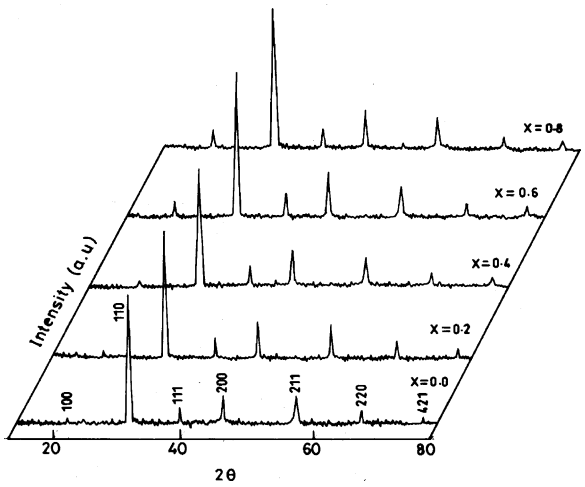

Fig. 1. X-ray diffraction patterns of $La_xSr_{1-x}FeO_3$.

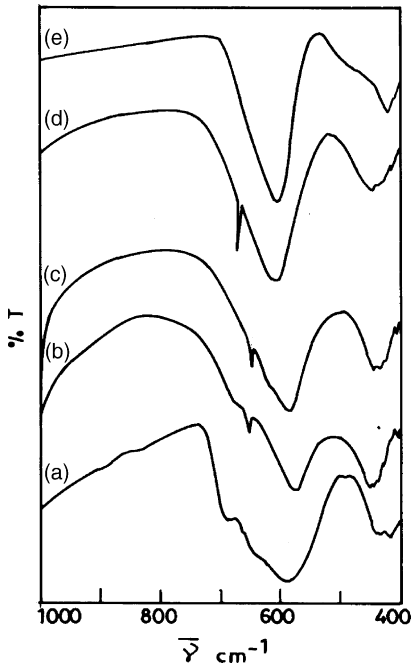

Fig. 2. FTIR spectra of $La_xSr_{1-x}FeO_3$; (a) $x = 0.0$, (b) $x = 0.2$, (c) $x = 0.4$, (d) $x = 0.6$ and (e) $x = 0.8$.

3. Results and discussion

3.1. Structural properties

Fig. 1 shows the X-ray diffraction patterns of the synthesized nanocrystalline $La_xSr_{1-x}FeO_3$ ($x = 0.0$, 0.2, 0.4, 0.6, 0.8) samples. The sharp well-defined peaks show the high crystalline nature of the synthesized compounds without any impure phase. All the peaks are matched well with the characteristic reflections of the parent compound. The XRD parameters, such as lattice constant, X-ray density, crystalline size and cell volume are given in Table 1. The lattice constant and cell volume have increased with increasing the molar substitution of La^{3+} on Sr^{2+} due to the difference in ionic radii (La^{3+} = 1.36 Å, Sr^{2+} = 1.25 Å). The observed lattice constant values are well agreed with the earlier reported values [9]. From the table the unsubstituted $SrFeO_3$ shows the formation of single-phase cubic structure. A phase transition from cubic to orthorhombic has been observed with increasing La^{3+} substitution. The sample $La_{0.6}Sr_{0.4}FeO_3$ has the crystalline size of 22 nm and was calculated from the X-ray line broadening method using Debye Scherror formula of $0.9\lambda/\beta\cos\theta$. Where, λ is the wavelength of the target CuKα 1.5406 Å, β the full width at half maximum of diffracted (1 1 0) plane. The X-ray density increases with increasing the substitution due to the difference in atomic concentration ($Sr = 1.78 \times 10^{22}$ cm^{-3} and $La = 2.7 \times 10^{22}$ cm^{-3}) [10].

The FTIR spectra of the nanocrystalline $La_xSr_{1-x}FeO_3$ ($x = 0.0$, 0.2, 0.4, 0.6, 0.8) are shown in Fig. 2 recorded at room temperature in the frequency range of 400–1000 cm^{-1}.

Table 1
XRD data of the synthesized compounds

Sample	Lattice constant			Cell volume (Å)	FWHM (θ)	Crystalline size (nm)	X-ray density (g cm^{-3})
	a (Å)	b (Å)	c (Å)				
$x = 0.0$	3.85	3.87	3.86	57.64	0.306	27	5.66
$x = 0.2$	5.44	5.82	7.71	244.7	0.306	27	6.08
$x = 0.4$	5.47	5.85	7.74	244.8	0.329	25	6.52
$x = 0.6$	5.49	5.85	7.78	250.5	0.376	22	6.98
$x = 0.8$	5.5	5.72	7.83	248.0	0.353	23	7.4

It is found that the spectra show two broad absorption bands in the range of 400–500 and 500–750 cm^{-1} which are attributed to BO_6 octahedron of stretching and bending vibrations of metal cations [11]. The FTIR spectra of $SrFeO_{3-\delta}$ shows two main absorption peaks at 587 and 420 cm^{-1}. The asymmetric higher frequency band ν_1 at 587 cm^{-1} may be attributed to the stretching vibrations of metal cations situated in the octahedral site i.e., Fe–O whereas the strong shoulders near 421.66 cm^{-1} can be attributed to the stretching vibrations of metal cation (Sr^{2+}) situated at the 12 coordinated position. It is well known that the cations in the octahedral site usually exhibit two IR active modes. The observed values of absorption peak values are well consistent with the previous literature [12]. The FTIR spectra for the $La_xSr_{1-x}FeO_{3-\delta}$ (where $x = 0.2$, 0.4, 0.6, 0.8) are shown in the Fig. 2b–e, respectively. From the figures it can be inferred that the compounds with lanthanum concentrations such as 0.4, 0.6, 0.8 M show a shifting of higher frequency band ν_1 from 605 to 593 cm^{-1} and one of the active mode of Fe–O stretching band around 660 cm^{-1} gets gradually more pronounced till La = 0.6 M. However the same band in the case of La = 0.8 M does not have any appreciable intensity which may be due to the increase in the concentration of lanthanum. It has also been noticed that the lower frequency band ν_2 gets shifted from 465 to 405 cm^{-1} resulting from the reduction in the oxygen vacancies in the samples with increasing lanthanum concentration, which is also evident from the diffusion coefficient calculations. These oxygen vacancies act as small grains whereas the substitution reduces the grain diameter, which eventually results in the shift from 465 to 405 cm^{-1}. It can also be attributed to the modification in the perovskite crystal structure due to the substitution of lanthanum with higher coordination (+3) in the place of strontium with lower coordination (+2) number. However in the sample $La_{0.2}Sr_{0.8}FeO_3$ the shoulder around 600 cm^{-1} gets shifted into multiple bands, which may be due to the mass disparity in the compound [13].

3.2. Physical properties

Density is one of the important physical parameters required for the assessment of new materials and one of the simplest parameter in verifying the new materials synthesis. Table 2 gives the density values calculated for the as synthesised flowery powder and the densities before and after sintering of the pure $SrFeO_{3-\delta}$. This also gives the flowery density and tap density of the powders as well as the densities before and after sintering of the compacts resulted for the specimen obtained by substitution of 0.2, 0.4, 0.6, 0.8 mol% of La^{3+}. It can be seen that the density of flowery powder is the lowest, which goes on increasing with the substitution of lanthanum. Similar observations are also made on the tap density of the powder. This may be due to the continued substitution of Sr^{2+} ions by La^{3+} ions with higher atomic mass. Similarly the densities of the compacts also found to increase with lanthanum substitution. The effect of temperature can be understood by comparing the density values of the compacts before and after sintering. It is seen that the values are higher for the sintered materials than the green material irrespective of the composition. Considering the overall values the lowest density obtained was 0.13 gm cm^{-3} for the $SrFeO_{3-\delta}$ flowery powder and the highest value of 3.78 gm cm^{-3} for $La_{0.8}Sr_{0.2}FeO_3$. The reasons for this minimum and maximum are obvious due to the increased mass contribution from the substitution. The increasing density observed during sintering may be due to the effect of temperature, which manifest in many ways. Firstly a consolidation of the loosely bound matter takes place by various diffusion processes and secondly different structural changes take place in consequence of the breaking and forming of different compounds. This has

Table 2
Density data of various compounds

Sample	Powder density		Pellet density	
	Flowery density (gm cm^{-3})	Tap density (gm cm^{-3})	Before sintering (gm cm^{-3})	After sintering (gm cm^{-3})
$SrFeO_{3-\delta}$	0.13	1.22	2.41	3.18
$La_{0.2}Sr_{0.8}FeO_{3-\delta}$	0.14	1.25	2.42	3.21
$La_{0.4}Sr_{0.6}FeO_{3-\delta}$	0.22	1.27	2.56	3.25
$La_{0.6}Sr_{0.4}FeO_{3-\delta}$	0.24	1.43	2.77	3.56
$La_{0.8}Sr_{0.2}FeO_{3-\delta}$	0.26	2.57	3.43	3.78

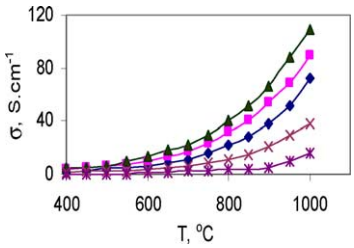

Fig. 3. Electrical conductivity vs. temperature for $La_xSr_{1-x}FeO_3$ (♦) $x = 0.0$, (■) $x = 0.2$, (▲) $x = 0.4$, (×) $x = 0.6$ and (✱) $x = 0.8$.

been affected by the diffusion of various constituent cations and anions into different regions. The process will also be marked by the formation of new compounds. By considering the oxides as simple spheres, the diffusion process is assumed to take place by the bringing up of spheres closer to one another, depending upon the attraction between the spheres. Hence either the separation or the closeness between the heading spheres always depends upon their fundamental characteristics. The increasing density may also be the result of decreased porosity. Porosity is the ratio of the voids volume to the total volume of the compacts. Hence it is understandable that with sintering, as temperature increases the number of voids or free volume or air packets inside the compacts decrease resulting a higher density.

3.3. Electrical properties

The temperature dependence of electrical conductivity of the series of samples $La_xSr_{1-x}FeO_3$ ($x = 0.0, 0.2, 0.4, 0.6, 0.8$) is given in Fig. 3. It can be seen that the conductivity increases with increase in temperature thereby indicating the materials to be of semiconducting nature. At lower temperature the conduction is due to electronic conduction whereas at higher temperature the conduction may be due to ionic conduction. The maximum conductivity of the undoped strontium ferrite was $72\ S\ cm^{-1}$, which is attributed to the highly abundant electrons formed during reduction [14] according to the following reaction

$$O_0^x \leftrightarrow V_0^{\bullet\bullet} + 2e^- + 0.5O_2 \quad (2)$$

As the concentration of La^{3+} substitution increases the conductivity also increases up to $x = 0.4$ and thereafter found to decrease. The maximum electrical conductivity of $109\ S\ cm^{-1}$ was observed for $La_{0.4}Sr_{0.6}FeO_3$ resulted from the contribution of the increased charge carriers due to the reaction

$$Sr^{2+} \Leftrightarrow La^{3+} + e^- \quad (3)$$

In compounds where $x \geq 0.6$ the conductivity value decreases due to the charge order of La^{3+}, Sr^{2+} that localizes the electrons and hence reduce the conductivity. Further, a decrease in the electron double exchange process caused by the increase in the cell volume and bond length M–O and Fe–O distance may decrease conductivity. The decrease in the conductivity may also be due to higher oxygen vacancy in the crystal lattice created by increased concentration of La^{3+} [15]. The electrical properties of $La_{1-x}Sr_xFeO_3$ have been elaborately studied by Patrakeev et al. [9]. The activation energies are calculated from the Arrhenius plots (Fig. 4) are tabulated in Table 3. From the table it is evident that many of the samples have higher activation energies and higher conduction at higher temperature, which may be due to the ionic conductivity predominant at higher temperature in the non-stoichiometric perovskite oxides [16]. The La^{3+} substitution also increases the conductivity up to $x = 0.4$, and thereafter decreases due to the high activation energy.

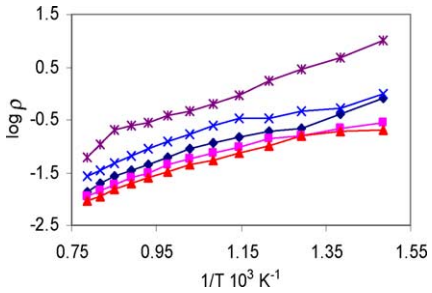

Fig. 4. Arrehenius plots for $La_xSr_{1-x}FeO_3$ (♦) $x = 0.0$, (■) $x = 0.2$, (▲) $x = 0.4$, (×) $x = 0.6$ and (✱) $x = 0.8$.

Table 3
Activation energies

Sample x	Activation energy	
	Low temp. (eV)	High temp. (eV)
0.0	0.61	0.59
0.2	0.23	0.64
0.4	0.11	0.57
0.6	0.17	0.71
0.8	0.54	1.23

The diffusion coefficient of oxygen vacancies in $La_xSr_{1-x}FeO_3$ ($x = 0.0, 0.2, 0.4, 0.6, 0.8$) as a function of reciprocal of temperature is shown in Fig. 5. The diffusion coefficient of oxygen vacancies [17] is calculated from the relation

$$D = \frac{\sigma K_B T}{Ne^2} \quad (4)$$

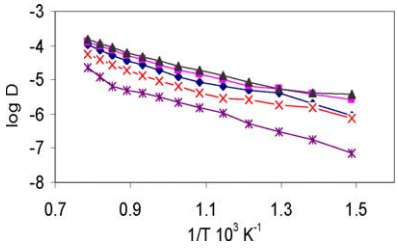

Fig. 5. Diffusion coefficient vs. reciprocal of temperature for $La_xSr_{1-x}FeO_3$ (♦) $x = 0.0$, (■) $x = 0.2$, (▲) $x = 0.4$, (×) $x = 0.6$ and (✱) $x = 0.8$.

where, σ is the electrical conductivity, K_B the Boltzman constant, T the measuring temperature, N the number of atoms $4 \times 10^{28}\,cm^{-2}$, e the electronic charge.

The study was helpful for analyzing the structural defects in the oxygen sublattice. From the figure it can be seen that the diffusion coefficient increases with the La^{3+} substitution up to $x = 0.4$ as well as with the temperatures. Therefore it is presumed that at higher temperature the ionic mobility is greatly enhanced. The non-stroichiometric strontium ferrite itself has some lattice vacancies due to the lack of oxygen content. The ionic diffusion may be produced due to the powder morphology, difference in ionic radii, and the number of vacancies in La^{3+}/Sr^{2+} sites [15]. At higher temperature the diffusion coefficient is increased due to the migration of ions from A-site to B-site or vice versa, resulting a higher conductivity by the gaining of external thermal energy. When the substitution $x \geq 0.6$ the compounds become more stoichiometric enabling better structural stability compared with parent compound hence the diffusion coefficient decreases. Due to the maximum oxygen vacancies and diffusion coefficient of the compounds $La_{0.4}Sr_{0.6}FeO_3$ gives the maximum electrical conductivity.

3.4. Electrochemical polarization studies

The electrochemical behaviors of $La_xSr_{1-x}FeO_3$ ($x = 0.0$, 0.2, 0.4, 0.6, 0.8) electrodes were studied in 1 and 2 M KOH solutions and the representative figure of 2 M solutions is given in Fig. 6. The calculated corrosion current density (I_{corr}), corrosion potential (E_{corr}), anodic and cathodic Tafel slopes (b_a and b_c) are tabulated in Table 4. It can be seen from the table the E_{corr} values are found to decrease with increase in concentration of La^{3+} ion up to $x = 0.4$ M and thereafter found to be increased. Similar observations are also made on the I_{corr} values. The minimum I_{corr} value of 0.001 mmpy was resulted for $Sr_{0.6}La_{0.4}FeO_3$ in 1 M KOH solutions. The reason behind the increasing I_{corr} value with increasing concentration ($x \geq 0.6$ M) may be due to the excess precipitation over the grain boundaries. The grain boundaries are considered to be high-energy regions and hence responsible for the anodic dissolution of the compounds which are weaker than the grains. Considering the b_a and b_c values in 1 M KOH solutions, the b_a values are found to decrease with increasing concentration of La^{3+} ion up to $x = 0.4$ M thereafter the values are increased. This reflects that the excess La^{3+} ion may cause enhanced anodic dissolution of the compound. A similar trend is also observed in the case of cathodic Tafel slope b_c. The b_c values of $-172\,mV\,dec^{-1}$ for $x = 0.0$ and $-47.4\,mV\,dec^{-1}$ for $x = 0.4$ M. The b_a values are found to be greater than the b_c values in most of the cases, hence the behavior of the studied materials are found to be under anodic control. The corrosion behaviors of these materials are predominantly governed by the oxygen evolution mechanism rather than the hydrogen evolution. According to Goodenough [18] the electrons are conducted to the empty σ^* band from the partially filled π^*_β band. Therefore it enhances the oxygen evolution reaction. The reaction mechanism of the oxygen evolution of the synthesized electrodes is as follows [19].

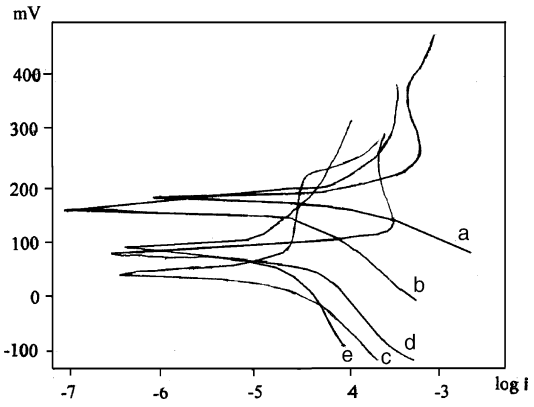

Fig. 6. Potentiostatic polarization of $La_xSr_{1-x}FeO_3$ (a) $x = 0.0$, (b) $x = 0.2$, (c) $x = 0.4$, (d) $x = 0.6$ and (e) $x = 0.8$ in 2 M KOH solutions.

$$M^z + OH^- \leftrightarrow M^z\text{–}OH + e^- \quad (6)$$

$$M^z\text{–}OH + OH^- \xrightarrow{rds} M^z\text{–}H_2O_2 + e^- \quad (7)$$

Table 4
Electrochemical parameters

$La_xSr_{1-x}FeO_3$	KOH conc. (M)	Electrochemical parameters				
		E ($i = 0$)	I_{corr} (mA cm^{-2})	b_a (mV)	b_c (mV)	Corr. rate (mmpy)
$x = 0.0$	1	127	0.1169	425	−172	1.368
	2	184	0.2383	591	−110	2.788
$x = 0.2$	1	069	0.0098	33.4	−107	0.115
	2	117	0.0272	175.	−173	0.318
$x = 0.4$	1	044	0.0001	67	−47	0.001
	2	070	0.0001	125	−155	0.002
$x = 0.6$	1	91	0.0016	91	−51	0.018
	2	98	0.0052	−281	−107	0.061
$x = 0.8$	1	99	0.1262	791	−243	1.476
	2	99	0.021	432	−563	0.252

$$(H_2O_2)_{phys} + OH^- \leftrightarrow (HO_2{}^-)_{phys} + H_2O \quad (8)$$

$$(H_2O_2)_{phys} + (HO_2{}^-)_{phys} \leftrightarrow H_2O + OH^- + O_2 \uparrow \quad (9)$$

Where, M^z is a transition metal ion with a valence state z^+at the surface of the perovskite.

Similar observations are also noticed in the case of 2 M KOH solutions. The corrosion rate of the materials is found to increase with increase in concentration of the electrolyte. Which may be due to the increase in concentration of OH^- ions. Generally, OH^- ions are assumed to be a highly corrosive species for oxide electrodes. From the above observations it may be concluded that the electrode $Sr_{0.6}La_{0.4}FeO_3$ is more stable and inhibits corrosion especially at lower concentration of KOH.

4. Conclusion

Citrate combustion method is found to be a simple and convenient method for the synthesis of new materials. The density of the substituted $SrFeO_{3-\delta}$ is observed to increase with La^{3+} substitution. Among the substituted ferrites the maximum specific electrical conductivity is noticed in $La_{0.4}Sr_{0.6}FeO_3$. From the activation energy values maximum beneficial effect of substitution is derived for $x = 0.4$ substitution. The maximum values of diffusion coefficient are noticed in $La_{0.4}Sr_{0.6}FeO_3$ coinciding well with conductivity measurements. XRD patterns show the synthesized $SrFeO_3$ materials have a cubic structure and the substituted compounds show orthorhombic structure. FTIR spectra show the characteristic peaks of substituted and unsubstituted ferrites. Considering the physical, electrical and electrochemical properties of the synthesized compounds the $La_{0.4}Sr_{0.6}FeO_3$ is assessed to be a suitable green electrode material for electrometallurgy applications.

Acknowledgement

The authors express their gratitude to The Director, CECRI, Staff of Electropyrometallurgy Division and Characterization laboratory for their kind help.

References

[1] K. Suresh, T.S. Panchapagesan, K.C. Patil, Solid State Ionics 126 (1999) 299.
[2] H. Kato, T. Kudo, H. Naito, H. Yugami, Solid Satate Ionics 159 (2003) 217.
[3] Y. Zhu, H. Wang, R. Tan, L. Cao, J. Alloys Compd. 352 (2003) 134.
[4] K. Suresh, K.C. Patil, in: K.J. Rao (Ed.), Perspectives in Solid State Chemistry, Narosa Publication, New Delhi, 1997, p. 376.
[5] R.N. Singh, B. Lal, Int. J. Hyd. Energy 27 (2002) 45.
[6] C.O. Augustin, L. John Berchmans, R. Kalai Selvan, Mater. Lett. 58 (2004) 1260.
[7] David Segel, J. Mater. Chem. 7 (1997) 1297.
[8] Xiwei Qi, Ji Zhou, Zhenxing Yue, Zhilun Gui, Longtu Li, Mater. Chem. Phys. 78 (2003) 25.
[9] M.V. Patrakeev, J.A. Banteeva, E.B. Mitberg, I.A. Leonidov, V.L. Kozhevnikov, K.R. Poeppelmeir, J. Solid State Chem. 172 (2003) 219.
[10] C. Kittel, Introduction to Solid State Physics, seventh ed., John Wiley Sons Inc., 1996, p. 24.
[11] J.P. Miao, L.P. Li, Y.B. Song, D.P. Xu, Z. Lu, W.H. Su, Mater. Chem. Phys. 62 (2000) 226.
[12] X. Li, H. Zhang, M. Zhang, Mater. Chem. Phys. 41 (1995) 41.
[13] R.D. Waldron, Phys. Rev. 99 (1955) 1727.
[14] F.W. Poulson, J. Lauvsted, R. Tunold, Solid Sate Ionics 72 (1994) 47.
[15] J.A.M. Van Roosmala, E.H.P. Coxafine, J.P.P. Huijsmanuy, Solid Sate Ionics 66 (1993) 285.
[16] J.W. Stevenson, K. Hasinska, N.L. Canfield, T.R. Armstrong, J. Electrochem. Soc. 147 (2000) 3213.
[17] O.M. Hemada, M.El. Saadaway, J. Magn. Magn. Mater. 256 (2003) 63.
[18] J.B. Goodenough, J. Appl. Phys. 37 (1966) 1415.
[19] L. Formaro, M. Longhi, J. Phys. Chem. B 107 (2003) 6425.